EFFECTS OF PRE-STRESS ON IMPACT WAVES IN AN INCOMPRESSIBLE ELASTIC PLATE

by H. A. ERBAY

(*Department of Mathematics, Istanbul Technical University, Maslak* 80626, *Istanbul, Turkey*)

Y. B. FU

(*Department of Mathematics, University of Keele, Staffordshire* ST5 5BG)

and G. A. ROGERSON

(*Department of Computer and Mathematical Sciences, Salford University, Salford* M5 4WT)

[Received 29 July 1999. Revise 21 February 2000]

Summary

We study the effects of pre-stress on the propagation of impact waves resulting from a sudden line load applied on the surface of an infinite isotropic incompressible elastic plate placed on a smooth rigid foundation. The pre-stress is assumed to be a uni-axial compression or an all-round pressure (tension). Our interest is in the behaviour of the impact waves when the pre-stress approaches any of the critical values for buckling instability. The problem is solved using Laplace and Fourier transforms. The Laplace inversion is carried out analytically and the Fourier inversion is evaluated both numerically and with the aid of the method of stationary phase.

1. Introduction

The main objective of the present work is to investigate the effects of pre-stress on the propagation of impact waves in an incompressible elastic plate. The response of an elastic plate to surface loads is mainly affected by the dispersive wave motions arising because of the existence of a natural length scale (the thickness of the plate). Since a full understanding of such surface load generated transient motions is important for practical applications, many researchers have investigated various aspects of impact problems. However, surprisingly little attention in the vast literature has been focused upon the effects of pre-stress on the transient response of elastic plates. This aspect is the main motivation for the present study.

The study of steady-state waves propagating in an infinite elastic plate goes back to Rayleigh and Lamb. A detailed analysis of the dispersion relation for Rayleigh–Lamb waves was presented in a monograph by Mindlin (**1**). Transient problems in elastic waveguides have been extensively studied in the literature because of their relevance to seismology, and a comprehensive account of early work can be found in the monographs by Miklowitz (**2**) and Achenbach (**3**). Generally speaking, apart from a fully numerical solution, three types of approaches have been used to study transient waves excited by impulsive forces: the method of generalized rays, the method of normal modes (that is, the method of eigenfunction expansion) and the transform methods (**4**). The method of generalized rays becomes impractical due to the fact that a very large number of generalized ray integrals must be evaluated numerically when the receiver is at a large distance, for example, greater than 10 plate thicknesses. In their application of the method of normal mode or eigenfunction expansion,

 © Oxford University Press 2000

Weaver and Pao (**5**) used the eigenfunctions for a finite circular plate and then derived the results for the infinite plate by letting the radius of the plate become infinite. However, the mathematical justification, especially proof of convergence, of this approach remains an unsolved task. In the transform method, which is the technique used in the present study and in Green and Green (**6**) and Rogerson (**7**), the solution to the transient problem is expressed in terms of Laplace and Fourier transform integrals. The inverse transformation integrals are then evaluated either numerically or by asymptotic techniques. In this paper, the Laplace inversion is carried out using the calculus of residues and the Fourier inversion is carried out both numerically and with the aid of the method of stationary phase.

Among the studies which have relevance to the present work we cite the paper by Jones (**8**), which is concerned with plane-strain flexural waves in an elastic layer. Using the method of stationary phase, Jones derived asymptotic expressions for the stress components at the upper surface of the plate and made valuable contributions to that problem in the case of finite stationary phase points. In the present paper, the results given in (**8**) will be extended to the case where an initial stress exists. It is known that as the wavenumber increases, the group velocity of the lowest mode approaches the velocity of the associated Rayleigh surface wave while the group velocities of the higher modes approach the velocity of shear waves. Within the context of the method of stationary phase, the Rayleigh wavefront and shear wavefront correspond to stationary phase points at positive infinity. In a recent paper, Dai and Wong (**9**) pointed out that the calculations made by Jones (**8**) for the stationary phase points at infinity were in error, and they presented an asymptotic expression for the shear-wave front.

This paper is organized as follows. In section 2, we present the basic equations for a pre-stressed, incompressible elastic plate. The derivation of the equations of motion closely follows the studies by Ogden and Roxburgh (**10**) where the dispersion relation of a pre-stressed elastic plate is derived and is studied in detail for particular forms of the strain energy function and by Rogerson and Fu (**11**) where a full asymptotic analysis of the dispersion relation is carried out for both short and long wavelength limits and for high mode numbers.

In section 3, the impact problem is formulated and is solved by using an integral transform formulation. Specifically, a Fourier transform is taken with respect to the horizontal space coordinate and Laplace transform with respect to time. The Laplace inversion is carried out with the aid of the calculus of residues and the horizontal and vertical displacement components are then expressed as two integrals arising from subsequent Fourier inversion.

In section 4 the application of the method of stationary phase to the present problem is discussed, and in section 5 we evaluate the Fourier inversion integrals numerically. The two approaches are found to agree extremely well over their common region of validity. Results are presented for typical values of pre-stress. In the final section, we discuss our results and draw some conclusions.

2. Basic equations

We shall consider a homogeneous elastic body B composed of a non-heat-conducting elastic material which possesses an initial unstressed state B_0. A purely homogeneous static deformation is then imposed upon B_0 to produce a finitely stressed equilibrium configuration denoted by B_e. Finally, a small time-dependent motion is superimposed upon B_e, and this configuration, termed the current configuration, is denoted by B_t. The position vectors of a representative particle are denoted by X_A, $x_i(X_A)$ and $\tilde{x}_i(X_A, t)$ in B_0, B_e and B_t, respectively. The position vector $\tilde{x}_i(X_A, t)$ may

therefore be represented in the form

$$\tilde{x}_i(X_A, t) = x_i(X_A) + u_i(x_j, t), \tag{2.1}$$

within which $\mathbf{u}(\mathbf{x}, t)$ is a small time-dependent displacement associated with the deformation $B_e \to B_t$.

The deformation gradients arising from the deformations $B_0 \to B_t$ and $B_0 \to B_e$ are denoted by $\mathbf{F}$ and $\bar{\mathbf{F}}$ and defined by

$$F_{iA} = \frac{\partial \tilde{x}_i}{\partial X_A}, \quad \bar{F}_{iA} = \frac{\partial x_i}{\partial X_A}. \tag{2.2}$$

Equations (2.1) and (2.2) may now be employed to deduce that these two deformation gradients are related through

$$F_{iA} = (\delta_{ij} + u_{i,j})\bar{F}_{jA}, \tag{2.3}$$

where the comma indicates differentiation with respect to the implied spatial coordinate in B_e. Furthermore, the convention whereby upper case letters refer to coordinates in B_0 and lower case letters refer to coordinates in B_e will be strictly observed.

A restriction upon the class of elastic material considered is made by imposing the constraint of incompressibility, ensuring that every possible deformation is isochoric. This in turn may be shown to imply that

$$J - 1 = 0, \quad J = \det\mathbf{F}, \tag{2.4}$$

throughout every possible material motion. A condition such as (2.4) is usually referred to as an internal constraint. It is usual for problems involving internal constraints to introduce a pseudo strain energy function. In the case of incompressibility this function is of the form

$$W(\mathbf{F}) = W_0(\mathbf{F}) - p(J - 1). \tag{2.5}$$

In equation (2.5), W_0 generates the constitutive part of the stress, whilst the other term generates a workless reaction stress. This additional term is constrained to be zero throughout all deformations. For the constraint of incompressibility the scalar multiplier p is interpreted as a pressure and must ultimately be chosen so that all the equations of motion and any prescribed boundary conditions are satisfied. If we use $\bar{p}$ and p^* to denote the pressure in B_e and the time dependent incremental pressure, respectively, then

$$p = \bar{p} + p^*. \tag{2.6}$$

In the absence of body forces, the equations of motion are given by $\pi_{iA,A} = \rho_0 \ddot{u}_i$, where $\boldsymbol{\pi}$ is the first Piola–Kirchhoff stress which in component form is given by $\pi_{iA} = \partial W/\partial F_{iA}$, ρ_0 is the density per unit volume of B_0 and a superimposed dot indicates differentiation with respect to time. Upon invoking equation (2.5) $\boldsymbol{\pi}$ may be decomposed into its constitutive and reaction components, thus

$$\pi_{iA} = \frac{\partial W_0}{\partial F_{iA}} - pF^{-1}_{Ai}. \tag{2.7}$$

Insertion of (2.7) into the equations of motion then gives

$$\left(\frac{\partial W_0}{\partial F_{iA}}\bar{F}_{jA} - pF^{-1}_{Ai}\bar{F}_{jA}\right)_{,j} = \rho_0 \ddot{u}_i. \tag{2.8}$$

To obtain the linearized form of the above equation of motion, we expand $\partial W_0/\partial F_{iA}$ into a Taylor series about $F_{iA} = \bar{F}_{iA}$ and make use of (2.3) and (2.6). After neglecting nonlinear terms, we obtain

$$\mathcal{A}_{jilk} u_{k,lj} - p^*_{,i} = \rho_0 \ddot{u}_i, \tag{2.9}$$

where $\mathcal{A}_{jilk}$, defined by

$$\mathcal{A}_{jilk} = \bar{F}_{jA}\bar{F}_{lC} \frac{\partial^2 W_0}{\partial F_{iA}\partial F_{kC}}|_{\mathbf{F}=\bar{\mathbf{F}}}, \tag{2.10}$$

is the first-order tensor of instantaneous elastic moduli. In obtaining (2.9), we have also used the relation $u_{p,p} = 0$ which is the linearized form of $(2.4)_1$.

We now proceed to obtain the linearized surface tractions. If we assume that the normals to a material surface in B_0 and B_e are given by N_A and n_i, respectively, then

$$\mathbf{N} dA = \bar{\mathbf{F}}^T \mathbf{n} da, \tag{2.11}$$

where da and dA are elements of area in B_e and B_0, respectively; see Chadwick (**12**). Then $T_i^{\mathbf{n}}$, the incremental surface traction per unit area in B_e, can be written as

$$T_i^{\mathbf{n}} = (\pi_{iA} - \bar{\pi}_{iA}) N_A \frac{dA}{da}, \tag{2.12}$$

where $\bar{\pi}_{iA}$ is the value of π_{iA} when $\mathbf{F} = \bar{\mathbf{F}}$ and $p = \bar{p}$ and the superscript $\mathbf{n}$ signifies the fact that $T_i^{\mathbf{n}}$ is the traction on a surface which has outward unit normal $\mathbf{n}$ in B_e. On substituting (2.7) and (2.11) into (2.12), expanding π_{iA} into a Taylor series about $F_{iA} = \bar{F}_{iA}$, $p = \bar{p}$, making use of (2.3), (2.6) and (2.10) and finally neglecting nonlinear terms, we arrive at the following measure of linearized incremental surface tractions:

$$T_i^{\mathbf{n}} = \mathcal{A}_{jilk} u_{k,l} n_j + \bar{p} u_{j,i} n_j - p^* n_i. \tag{2.13}$$

Before proceeding further we shall discuss the expression of the initial stress in B_e in terms of the principal stretches. For the Cauchy stress we have

$$\bar{\boldsymbol{\sigma}} = \mathrm{diag}(\sigma_1, \sigma_2, \sigma_3), \qquad \sigma_i = \lambda_i \frac{\partial W_0}{\partial \lambda_i} - \bar{p}, \tag{2.14}$$

where λ_i $(i = 1, 2, 3)$ are the three principal stretches associated with the deformation $B_0 \to B_e$ and there is no implied summation on i. For a neo-Hookean material,

$$W_0 = \tfrac{1}{2}\mu(\mathrm{tr}\mathbf{B} - 3) = \tfrac{1}{2}\mu(\lambda_1^2 + \lambda_2^2 + \lambda_3^2 - 3),$$

where $\mathbf{B} = \mathbf{F}\mathbf{F}^T$ and μ is the shear modulus. We then have

$$\mathcal{A}_{jilk} = \mu \bar{B}_{jl}\delta_{ik}, \quad \sigma_i = \mu\lambda_i^2 - \bar{p}, \tag{2.15}$$

where $\bar{\mathbf{B}} = \bar{\mathbf{F}}\bar{\mathbf{F}}^T$. For expressions of $\mathcal{A}_{jilk}$ in terms of the principal stretches for general strain energy functions, we refer the reader to the book by Ogden (**13**).

3. Transient motion of an incompressible elastic plate

We shall now consider transient waves in an incompressible elastic plate which is pre-stressed, placed on a rigid smooth foundation and of thickness h in B_e. We choose a Cartesian coordinate system which coincides with the principal axes of stress in B_e. The origin O is located at the bottom surface, the x_1- and x_2-axes are chosen so that Ox_2 is normal to the plane of the plate and therefore the upper and lower surfaces of the plate are the planes at $x_2 = 0, h$. In order to simplify the governing equations a state of plane strain is assumed so that $u_3 \equiv 0$ and both u_1 and u_2 are independent of x_3. The linearized incompressibility condition and the two non-trivial equations of motion then take the following form:

$$u_{1,1} + u_{2,2} = 0, \tag{3.1}$$

$$\mathcal{A}_{jilk} u_{k,lj} - p^*_{,i} = \rho_0 \ddot{u}_i, \qquad i = 1, 2. \tag{3.2}$$

In view of the simplified incompressibility condition (3.1), we may introduce a 'stream' function $\psi(x_1, x_2, t)$ such that $u_1 = \psi_{,2}$ and $u_2 = -\psi_{,1}$. Substituting these expressions into (3.2) and then eliminating the incremental pressure p^* by cross differentiation, we obtain a single equation for ψ:

$$\alpha\psi_{,1111} + 2\beta\psi_{,1122} + \gamma\psi_{,2222} = \rho_0 \nabla^2 \ddot{\psi}, \tag{3.3}$$

where

$$\alpha = \mathcal{A}_{1212}, \quad 2\beta = \mathcal{A}_{1111} + \mathcal{A}_{2222} - 2\mathcal{A}_{1122} - 2\mathcal{A}_{1221}, \quad \gamma = \mathcal{A}_{2121}.$$

The incremental tractions on the two surfaces $x_2 = 0, h$ are given by $-T_i(x_1, 0, t)$ and $T_i(x_1, h, t)$, respectively, where from (2.13),

$$T_i(x_1, x_2, t) = \mathcal{A}_{2ilk} u_{k,l} + \bar{p} u_{2,i} - p^* \delta_{2i}. \tag{3.4}$$

The p^* can be eliminated from (3.4) when $i = 2$ by differentiating this equation with respect to x_1 and using (3.2) for $p^*_{,1}$. We then have

$$\begin{aligned} T_1 &= (\sigma_2 - \gamma)\psi_{,11} + \gamma\psi_{,22}, \\ T_{2,1} &= \rho_0 \ddot{\psi}_{,2} - (2\beta + \gamma - \sigma_2)\psi_{,112} - \gamma\psi_{,222}, \end{aligned} \tag{3.5}$$

where we have used $(2.15)_2$ and the relation

$$\lambda_2 \frac{\partial W_0}{\partial \lambda_2} = \sigma_2 + \bar{p} = \mathcal{A}_{2121} - \mathcal{A}_{2112}$$

to eliminate $\bar{p}$ in favour of σ_2 (see **13**). Similar approaches have been followed in Ogden and Roxburgh (**10**) and Rogerson and Fu (**11**).

It is convenient to non-dimensionalize the governing equations and boundary conditions by scaling x_i and u_i by h, ψ by h^2, α, β, γ, σ_2, T_1 and T_2 by μ and t by $h(\rho_0/\mu)^{\frac{1}{2}}$. Using the same symbols to denote the new dimensionless variables, we see that the dimensionless governing equations are again (3.1) to (3.5) but with $\mu = \rho_0 = h = 1$.

Furthermore, in order to reduce the complexity of the equations to be obtained we assume that the material constants α, β and γ satisfy the following restriction:

$$\gamma + \alpha = 2\beta. \tag{3.6}$$

This relation holds as an identity for neo-Hookean and Mooney–Rivlin materials.

Before proceeding to the impact problem, we shall summarize the main results concerning the propagation of travelling waves in the pre-stressed plate described above. These results provide the necessary basis for our later analysis. Travelling wave solutions are governed by (3.3) together with the dead-load boundary conditions $T_1 = 0$, $T_2 = 0$ on $x_2 = 1$ and $T_1 = 0$, $u_2 = 0$ on $x_2 = 0$. For a travelling wave the function ψ is assumed to have the normal form $\psi = H(x_2)\exp\{ik(x_1 - vt)\}$, where k is the wavenumber and v is the wave speed. On substituting this expression into (3.3) and the four boundary conditions, we obtain an eigenvalue problem for $H(x_2)$ which can be solved to determine the dispersion relation between v and k and $H(x_2)$ to within an arbitrary constant. It can be shown (see, for example, (**10**) or (**11**)) that the dispersion relation is given by

$$(2\beta - \sigma_2 - v^2)^2 \tanh(qk) = (2\gamma - \sigma_2)^2 q \tanh(k), \tag{3.7}$$

where $q = ((\alpha - v^2)/\gamma)^{\frac{1}{2}}$ or $i((v^2 - \alpha)/\gamma)^{\frac{1}{2}}$ depending on whether $\alpha - v^2$ is positive or otherwise. We note that this is in fact the dispersion relation for extensional waves which can propagate in a plate which is subjected to the same pre-stress as above but has thickness $2h$ and boundary conditions $T_1 = T_2 = 0$ on both surfaces. This dispersion relation has an infinite number of branches. By considering the solutions of (3.7) when $v^2 = 0$, it can be shown that only the fundamental mode can be made marginally stable. When $v^2 = 0$, the corresponding relation between k and the pre-stress is called the *bifurcation condition*. It depends on the form of pre-stress. In this paper, two types of pre-stress will be considered.

All round pressure or tension

In this case no deformation is induced by the pre-stress due to constraint of incompressibility. We have $\alpha = \beta = \gamma = 1$ independent of material constitution. Equation (3.7) with $v^2 = 0$ becomes an identity. The bifurcation condition can be obtained by first expanding (3.7) for small v and then equating the coefficients of v. We have

$$\sigma_2^+ = 2, \qquad \sigma_2^- = -\frac{2\{\sinh(2k) + 2k\}}{\sinh(2k) - 2k}, \tag{3.8}$$

where we have used $+$ and $-$ to distinguish the two solutions (upper and lower branches of the stability curves). The v^2 for the fundamental mode is positive only if $\sigma_2^- < \sigma_2 < \sigma_2^+$. For values of σ_2 outside this stability range, linear theory predicts that normal mode perturbations applied to such a plate will grow exponentially (if $\sigma_2 \neq \sigma_2^+$ or σ_2^-) or algebraically (if $\sigma_2 = \sigma_2^+$ or σ_2^-). However, nonlinear effects come into play when the growth reaches a significant magnitude. It was shown in Fu and Rogerson (**14**) that when $\sigma_2 \approx \sigma_2^-$, nonlinearity has a stabilizing effect on moderate and large wavelength perturbations and has a destabilizing effect on small wavelength perturbations. For $\sigma_2 \approx \sigma_2^+$, the plate behaves like a non-dispersive medium, and for this case Fu (**15**) showed that nonlinearity exerts a stabilizing effect. Both studies are for neo-Hookean materials.

Uni-axial compression or tension along x_1-direction

In this case the bifurcation condition is dependent on material constitution. We assume that the composing material is neo-Hookean. Denoting the principal stretches along the x_1- and x_2-directions by λ and λ^{-1}, respectively, we have

$$\alpha = \lambda^2, \quad \gamma = \lambda^{-2}, \quad \sigma_2 = 0. \tag{3.9}$$

With the use of these relations, (3.7) with $v^2 = 0$ reduces to

$$4\lambda^2 \tanh(k) = (1 + \lambda^4)^2 \tanh(\lambda^2 k). \tag{3.10}$$

An explicit expression for λ in terms of k is not possible, but a simple numerical calculation shows that for each k this bifurcation condition has a single root for λ, and the latter is less than unity for all k, implying that a neo-Hookean plate can lose stability only if it is compressed. The single bifurcation curve, denoted by $\lambda = f(k)$ say, is monotone increasing: it cuts the k axis at $k = 3{\cdot}997$ and approaches $\lambda = 0{\cdot}544$ as $k \to \infty$, v^2 being positive only if $\lambda > f(k)$. Outside this stability range, linear theory predicts exponential or algebraic growth. But Fu and Ogden (**16**) showed that nonlinearity will stabilize any growing perturbations.

The dispersion curve determined by (3.7) has an infinite number of branches. In the numerical solution of the impact problem to be discussed later, the k axis is discretized and we need the values of v^2 on these branches at the discretizing points. We first determine the values v^2 at a starting point (chosen to be $k = 0{\cdot}01$ in our later numerical calculation) using the bisection method and then use the Newton–Raphson method to determine the values of v^2 along each branch. Difficulty can arise when q is close to zero. When this happens, the bisection method is used near the problem points.

We now proceed to consider the problem in which a line load is applied instantaneously to the upper surface of the plate. In other words we have the following boundary conditions:

$$\begin{aligned} &T_1 = 0, \qquad T_2 = -H(t)\delta(x_1) \quad \text{on} \quad x_2 = 1, \\ &T_1 = u_2 = 0 \quad \text{on} \quad x_2 = 0, \end{aligned} \tag{3.11}$$

where $H(t)$ is the Heaviside function and $\delta(x_1)$ is the usual delta function.

Equations (3.3), (3.5) and (3.11) form an initial-boundary-value problem which can be solved by applying Fourier transform with respect to x_1 and the one-sided Laplace transform with respect to t. To this end, we define $\hat{f}(s, k, x_2)$ as the Fourier–Laplace transform of function $f(t, x_1, x_2)$ through

$$\hat{f}(s, k, x_2) = \int_{-\infty}^{\infty} e^{ikx_1} \int_0^{\infty} f(t, x_1, x_2) e^{-st} dt dx_1, \tag{3.12}$$

where k and s are the variables of Fourier transform and Laplace transform, respectively. On taking the transforms of (3.3), (3.5) and (3.11), we obtain

$$\begin{aligned} &\hat{u}_1 = \hat{\psi}', \qquad \hat{u}_2 = ik\hat{\psi}, \\ &\hat{T}_1 = \gamma\hat{\psi}'' - k^2(\sigma_2 - \gamma)\hat{\psi}, \\ &ik\hat{T}_2 = \gamma\hat{\psi}''' - [s^2 + k^2(2\beta + \gamma - \sigma_2)]\hat{\psi}', \\ &\gamma\hat{\psi}'''' - (2\beta k^2 + s^2)\hat{\psi}'' + (\alpha k^4 + k^2 s^2)\hat{\psi} = 0, \end{aligned} \tag{3.13}$$

and

$$\begin{aligned} &\hat{T}_1 = 0, \qquad \hat{T}_2 = -1/s \quad \text{on} \quad x_2 = 1, \\ &\hat{T}_1 = \hat{\psi} = 0 \quad \text{on} \quad x_2 = 0, \end{aligned} \tag{3.14}$$

where a prime denotes differentiation with respect to x_2.

We now seek a solution of the equation of motion $(3.13)_5$ in the form $\hat{\psi} \sim \exp(\tilde{q}kx_2)$. If this form of solution is inserted into the equation of motion $(3.13)_5$, it is found that $\tilde{q}$ must satisfy the equation

$$\gamma\tilde{q}^4 - (2\beta + \hat{s}^2)\tilde{q}^2 + (\alpha + \hat{s}^2) = 0, \tag{3.15}$$

where $\hat{s} = s/k$. With the use of (3.6), the two roots for $\tilde{q}^2$ are found to be given by

$$\tilde{q}^2 = 1, \qquad \tilde{q}^2 = (\alpha + \hat{s}^2)/\gamma \equiv q^2. \tag{3.16}$$

The function $\hat{\psi}$ then takes the form

$$\hat{\psi} = A\cosh(kx_2) + B\sinh(kx_2) + C\cosh(qkx_2) + D\sinh(qkx_2), \tag{3.17}$$

where A, B, C, D are disposable constants. On substituting this expression into the boundary conditions (3.14) and solving the four resulting linear equations, we obtain $A = C = 0$ and

$$B = \frac{i}{k^2 s\Gamma(s,k)}(2\beta + \hat{s}^2 - \sigma_2)\sinh(kq), \quad D = -\frac{i}{k^2 s\Gamma(s,k)}(2\gamma - \sigma_2)\sinh(k), \tag{3.18}$$

where

$$\Gamma(s,k) = (2\beta + \hat{s}^2 - \sigma_2)^2\sinh(kq)\cosh(k) - q(2\gamma - \sigma_2)^2\sinh(k)\cosh(kq). \tag{3.19}$$

We note that as expected $\Gamma(ikv, k) = 0$ yields the dispersion relation (3.7). On substituting the above solution for $\hat{\psi}$ into (3.13a, b), we obtain

$$\hat{u}_1 = -\frac{i\Gamma_1(s,k,x_2)}{ks\Gamma(s,k)}, \quad \hat{u}_2 = \frac{\Gamma_2(s,k,x_2)}{ks\Gamma(s,k)}, \tag{3.20}$$

where

$$\begin{aligned}\Gamma_1(s,k,x_2) &= (2\gamma - \sigma_2)q\sinh(k)\cosh(kqx_2) - (2\beta - \sigma_2 + \hat{s}^2)\sinh(kq)\cosh(kx_2),\\ \Gamma_2(s,k,x_2) &= (2\gamma - \sigma_2)\sinh(k)\sinh(kqx_2) - (2\beta - \sigma_2 + \hat{s}^2)\sinh(kq)\sinh(kx_2).\end{aligned} \tag{3.21}$$

Equations (3.20) give the transforms of the horizontal and vertical displacements throughout the plate in terms of the two transform variables s and k at any x_2. In order to recover the dependence on t and x_1, these transforms must be inverted. The inversion procedure is similar to that in the classical case without pre-stresses. The inversion integrals for $\hat{u}_1$ and $\hat{u}_2$ are

$$\begin{aligned}u_1(t,x_1,x_2) &= -\frac{1}{4\pi^2}\int_{-\infty}^{\infty} e^{-ikx_1}dk \int_{c-i\infty}^{c+i\infty} \frac{\Gamma_1(s,k,x_2)}{ks\Gamma(s,k)}e^{st}ds,\\ u_2(t,x_1,x_2) &= \frac{1}{4\pi^2 i}\int_{-\infty}^{\infty} e^{-ikx_1}dk \int_{c-i\infty}^{c+i\infty} \frac{\Gamma_2(s,k,x_2)}{ks\Gamma(s,k)}e^{st}ds,\end{aligned} \tag{3.22}$$

where c is chosen such that all the singular points of the integrand lie on the left of the vertical line $s = c$ in the complex s-plane.

The integrals with respect to s may be evaluated in terms of the residues of the integrands. The poles of the integrands are $s = 0$ and the zeros of $\Gamma(s,k)$. By introducing the substitution $s = i\omega$ we reach the equation $\Gamma(i\omega, k) = 0$ which is the dispersion relation for travelling waves. For every value of k, this equation has an infinite number of pairs of roots in the form $\omega_n = \pm\omega_n(k)$ $(n = 1, 2, ...)$, each pair corresponding to forward and backward travelling waves associated with one branch of the dispersion curve for the wavenumber that is considered. The inverse Laplace transform can now be evaluated exactly and equations (3.22) become

$$\begin{aligned}u_1(t,x_1,x_2) &= u_1^{(0)} - \frac{i}{2\pi}\int_{-\infty}^{\infty} e^{-ikx_1}\sum_{n=1}^{\infty}\left[\left(\frac{e^{st}\Gamma_1}{s\partial\Gamma/\partial\hat{s}}\right)_{s=i\omega_n} + \left(\frac{e^{st}\Gamma_1}{s\partial\Gamma/\partial\hat{s}}\right)_{s=-i\omega_n}\right]dk,\\ u_2(t,x_1,x_2) &= u_2^{(0)} + \frac{1}{2\pi}\int_{-\infty}^{\infty} e^{-ikx_1}\sum_{n=1}^{\infty}\left[\left(\frac{e^{st}\Gamma_2}{s\partial\Gamma/\partial\hat{s}}\right)_{s=i\omega_n} + \left(\frac{e^{st}\Gamma_2}{s\partial\Gamma/\partial\hat{s}}\right)_{s=-i\omega_n}\right]dk,\end{aligned} \tag{3.23}$$

where $u_1^{(0)}$ and $u_2^{(0)}$, given by

$$u_1^{(0)} = -\frac{i}{2\pi}\int_{-\infty}^{\infty} e^{-ikx_1}\left(\frac{\Gamma_1}{k\Gamma}\right)_{s=0} dk, \quad u_2^{(0)} = \frac{1}{2\pi}\int_{-\infty}^{\infty} e^{-ikx_1}\left(\frac{\Gamma_2}{k\Gamma}\right)_{s=0} dk, \tag{3.24}$$

are contributions from the pole $s = 0$ and are the displacement field corresponding to a static line load.

The fact that Γ_1, Γ_2 and Γ are even functions of $\hat{s}$ $(= s/k)$ may now be used to write equation (3.23) in the simplified form

$$\begin{aligned} u_1(t, x_1, x_2) &= u_1^{(0)} + \frac{i}{\pi}\int_{-\infty}^{\infty} e^{-ikx_1}\sum_{n=1}^{\infty} M_n^{(1)}(i\omega_n, k, x_2)\cos\omega_n t\, dk, \\ u_2(t, x_1, x_2) &= u_2^{(0)} - \frac{1}{\pi}\int_{-\infty}^{\infty} e^{-ikx_1}\sum_{n=1}^{\infty} M_n^{(2)}(i\omega_n, k, x_2)\cos\omega_n t\, dk, \end{aligned} \tag{3.25}$$

where

$$M_n^{(1)}(i\omega_n, k, x_2) = -\left(\frac{\Gamma_1}{s\partial\Gamma/\partial\hat{s}}\right)_{s=i\omega_n}, \quad M_n^{(2)}(i\omega_n, k, x_2) = -\left(\frac{\Gamma_2}{s\partial\Gamma/\partial\hat{s}}\right)_{s=i\omega_n}. \tag{3.26}$$

Finally, it may also be shown that the horizontal modal function $M_n^{(1)}(i\omega_n, k, x_2)$ is an odd function of k whereas the vertical modal function $M_n^{(2)}(i\omega_n, k, x_2)$ is an even function of k. Thus, equations (3.25) may further be simplified to give

$$\begin{aligned} u_1(t, x_1, x_2) &= u_1^{(0)} + \frac{2}{\pi}\int_0^{\infty}\sum_{n=1}^{\infty} M_n^{(1)}(i\omega_n, k, x_2)\cos\omega_n t\sin kx_1\, dk, \\ u_2(t, x_1, x_2) &= u_2^{(0)} - \frac{2}{\pi}\int_0^{\infty}\sum_{n=1}^{\infty} M_n^{(2)}(i\omega_n, k, x_2)\cos\omega_n t\cos kx_1\, dk. \end{aligned} \tag{3.27}$$

A similar argument applied to (3.24) leads to

$$u_1^{(0)} = -\frac{1}{\pi}\int_0^{\infty}\left(\frac{\Gamma_1}{\Gamma}\right)_{s=0}\frac{\sin kx_1}{k}dk, \quad u_2^{(0)} = \frac{1}{\pi}\int_0^{\infty}\left(\frac{\Gamma_2}{\Gamma}\right)_{s=0}\frac{\cos kx_1}{k}dk. \tag{3.28}$$

The integrations in equations (3.27) are carried out along each branch of the dispersion curve which has an infinite number of branches. When $x_2 \neq 0, 1$, the modal functions in the integrands all tend to zero exponentially as $k \to \infty$ and an efficient numerical code can be written to evaluate the integrals by replacing the upper limit ∞ by a suitably large finite value. However, on the plate surface $x_2 = 1$, which is usually of most interest, the modal functions $M_n^{(1)}$ and $M_n^{(2)}$ for the harmonics tend to zero algebraically like $1/k^3$, whereas for the fundamental mode it can be shown with the aid of the asymptotic results given in Rogerson and Fu (**11**) that these modal functions have the following behaviour:

$$M_1^{(1)}(i\omega_1, k, 1) = \frac{q_R\gamma}{v_R^2}\cdot\frac{(2\gamma - \sigma_2)q_R - 2\beta + \sigma_2 + v_R^2}{4q_R\gamma(2\beta - \sigma_2 - v_R^2) - (2\gamma - \sigma_2)^2}\cdot\frac{1}{k} + \cdots, \tag{3.29}$$

$$M_1^{(2)}(i\omega_1, k, 1) = \frac{q_R\gamma}{v_R^2} \cdot \frac{v_R^2 - \alpha + \gamma}{4q_R\gamma(2\beta - \sigma_2 - v_R^2) - (2\gamma - \sigma_2)^2} \cdot \frac{1}{k} + \cdots, \tag{3.30}$$

where $q_R = ((\alpha - v_R^2)/\gamma)^{\frac{1}{2}}$, v_R being the Rayleigh wave speed. The neglected terms in the above expressions are exponentially small. It then follows that the integrand in $(3.27)_2$ corresponding to $n = 1$ behaves like

$$\frac{1}{k}\cos k v_R t \cos k x_1 = \frac{1}{2k}\{\cos k(x_1 - v_R t) + \cos k(x_1 + v_R t)\}$$

as $k \to \infty$. Therefore the integral in $(3.27)_2$ is convergent for all values of x_1 except $x_1 = v_R t$ which corresponds to the Rayleigh wavefront.

4. The method of stationary phase

Classical asymptotic methods such as the method of stationary phase, the method of steepest descent and the saddle point method have been found to be powerful tools in the study of general wave motion. The method of stationary phase provides an approximation describing the long time behaviour of the integrals such as those obtained in the preceding section. According to the method, the major contribution to the integrals arises from the vicinity of those points at which the phase function is stationary. This method will now be applied to evaluate the integrals of the preceding section, following the approach presented in Achenbach (**3**), and for a full description of the method the reader is referred to the book by Wong (**17**).

We first truncate the infinite summations in (3.25) by including only N branches and write (3.25) in the following form:

$$u_1(t, x_1, x_2) = u_1^{(0)} + \frac{i}{2\pi}\sum_{n=1}^{N}(I_{1n} + I_{2n}), \qquad u_2(t, x_1, x_2) = u_2^{(0)} - \frac{1}{2\pi}\sum_{n=1}^{N}(J_{1n} + J_{2n}), \tag{4.1}$$

where

$$\begin{aligned} I_{1n} &= \int_{-\infty}^{\infty} M_n^{(1)}(i\omega_n, k, x_2)e^{it\theta_1(k)}dk, \qquad I_{2n} = \int_{-\infty}^{\infty} M_n^{(1)}(i\omega_n, k, x_2)e^{-it\theta_2(k)}dk, \\ J_{1n} &= \int_{-\infty}^{\infty} M_n^{(2)}(i\omega_n, k, x_2)e^{it\theta_1(k)}dk, \qquad J_{2n} = \int_{-\infty}^{\infty} M_n^{(2)}(i\omega_n, k, x_2)e^{-it\theta_2(k)}dk, \end{aligned} \tag{4.2}$$

in which

$$\theta_1(k) = \omega_n - \frac{x_1}{t}k, \qquad \theta_2(k) = \omega_n + \frac{x_1}{t}k. \tag{4.3}$$

Recognize that if t is large, the oscillations of the purely oscillatory terms $\exp(it\theta_1(k))$ and $\exp(-it\theta_2(k))$ are very dense. Thus, in the above integrations, for t large enough, the positive and negative parts of the oscillations effectively cancel each other out, except in the vicinity of the stationary phase points, that is, the points where $\theta_1'(k) = 0$ and $\theta_2'(k) = 0$, where $'$ denotes differentiation with respect to k. That the major contribution to the integrals comes from the vicinity of the stationary phase points, or equivalently, that the integrals as $t \longrightarrow \infty$ is asymptotically equal to the integrals only over a small neighbourhood of the stationary phase points is the basic idea of the stationary phase approximation. Using equation (4.3), the stationary phase condition $\theta_1'(k) = 0$ can be expressed as

$$c_{gn} = x_1/t, \tag{4.4}$$

where $c_{gn} = d\omega_n/dk$ is the group velocity of the nth mode. We fix time t in our calculations. For each x_1, the wavenumbers satisfying equation (4.4) are determined. Suppose that there is one such finite value of k, ξ say. Then to leading order, the $M_n^{(1)}$ in I_{1n} can be evaluated at $k = \xi$ and $\theta_1(k)$ can be replaced by $\theta_1(\xi) + \frac{1}{2}\theta_1''(\xi)(k-\xi)^2$. Changing the integrating path to $k = \xi + \rho e^{\pm i\pi/4}$ $(-\infty < \rho < \infty)$ and using $\int_0^\infty \exp(-u^2)du = \sqrt{\pi}/2$, we obtain

$$I_{1n} \sim \left[\frac{2\pi}{t|\theta_1''(\xi)|}\right]^{1/2} M_n^{(1)}(i\omega_{n\xi},\ \xi,\ x_2)e^{i[\theta_1(\xi)t \pm \pi/4]}, \tag{4.5}$$

where $\omega_{n\xi} = \omega_n(\xi)$, the positive and negative signs in the exponential correspond respectively to $\theta_1''(\xi) > 0$ and $\theta_1''(\xi) < 0$, and $\theta_1''(\xi) \neq 0$ is assumed. For certain values of x_1/t there may be more than one stationary phase point. In such cases, there will be a contribution of the form (4.5) from each stationary phase point, and the complete solution is obtained by summation. A completely analogous expression can be written for J_{1n} by exchanging $M_n^{(1)}$ in equation (4.5) with $M_n^{(2)}$. Since the group velocity is an odd function of k, if $k = \xi$ is a finite stationary phase point of $\theta_1(k)$ then $k = -\xi$ will be a finite stationary phase point for $-\theta_2(k)$. Therefore the integrals I_{2n} and J_{2n} can be evaluated in just the same manner as I_{1n} and J_{1n} in which $k = -\xi$ and $-\theta_2(k)$ instead of $k = \xi$ and $\theta_1(k)$ will be used in the corresponding expressions. Remembering that $\theta_1''(k) = \omega_n''(k)$ is an even function of k and $M_n^{(1)}(i\omega_n, k, x_2)$ is an odd function of k whereas $M_n^{(2)}(i\omega_n, k, x_2)$ is an even function of k, we can write from (4.1) the asymptotic approximations for the horizontal and vertical displacements as follows:

$$\begin{aligned} u_1(t, x_1, x_2) &\sim u_1^{(0)} - \frac{2}{\sqrt{2\pi t}} \sum_{n=1}^{N} \frac{1}{\sqrt{|\omega_n''(\xi)|}} M_n^{(1)}(i\omega_{n\xi}, \xi, x_2) \sin(\omega_{n\xi}t - \xi x_1 \pm \pi/4), \\ u_2(t, x_1, x_2) &\sim u_2^{(0)} - \frac{2}{\sqrt{2\pi t}} \sum_{n=1}^{N} \frac{1}{\sqrt{|\omega_n''(\xi)|}} M_n^{(2)}(i\omega_{n\xi}, \xi, x_2) \cos(\omega_{n\xi}t - \xi x_1 \pm \pi/4), \end{aligned} \tag{4.6}$$

where the positive and negative signs correspond respectively to $\omega_n''(\xi) > 0$ and $\omega_n''(\xi) < 0$. We recall that the summation here is over a finite number of the branches and each term in the summation will include a further summation over all the stationary phase points of the corresponding branch.

The above analysis shows that the contributions from finite stationary phase points to the displacements are proportional to $(t|\omega_n''(\xi)|)^{-1/2}$. However, the above approximation breaks down for the points where the group velocity is stationary, so that $\omega_n''(\xi) = 0$. These points correspond to wavefronts. Suppose that ξ is a finite value of k at which $\omega_n''(\xi) = 0$ but $\omega_n'''(\xi) \neq 0$. Then a wavefront appears at $x_1 = \omega_n'(\xi)t$. In a small neighbourhood of this wavefront, we may introduce a local variable $u = x_1 - \omega_n'(\xi)t$. Again to leading order we may evaluate the $M_n^{(1)}$ in I_{1n} at $k = \xi$, but now we replace $\theta_1(k)$ by $\theta_1(\xi) - (u/t)(k-\xi) + \frac{1}{6}\omega_n'''(\xi)(k-\xi)^3$. With the aid of the relation (see (**18**, p.447))

$$\int_0^\infty \cos(at^3 \pm xt)dt = \frac{\pi}{(3a)^{1/3}} \mathrm{Ai}\left\{\pm(3a)^{-1/3}x\right\},$$

where Ai is the standard Airy function, we obtain

$$I_{1n} \sim 2\pi \left[\frac{2}{t|\omega_n'''(\xi)|}\right]^{1/3} M_n^{(1)}(i\omega_{n\xi}, \xi, x_2) e^{i\theta_1(\xi)t} \mathrm{Ai}(\pm|w|), \tag{4.7}$$

where the positive and negative signs correspond to $\theta_1'(\xi)\omega_n'''(\xi) > 0$ and $\theta_1'(\xi)\omega_n'''(\xi) < 0$, respectively, and

$$|w| = \left[\frac{2}{|\omega_n'''(\xi)|}\right]^{1/3} |\theta_1'(\xi)| t^{2/3}. \tag{4.8}$$

The expression in (4.7) depends on x_1 through $\theta_1(\xi)$ and $\theta_1'(\xi)$, where $\theta_1(\xi) = \omega_n(\xi) - \xi x_1/t$ and $\theta_1'(\xi) = \omega_n'(\xi) - x_1/t$. Writing similar expressions for J_{1n}, I_{2n} and J_{2n} and following a similar approach to that leading to equation (4.6), we have the following expressions for the displacements:

$$\begin{aligned} u_1 &\sim u_1^{(0)} + 2[\frac{2}{t|\omega_n'''(\xi)|}]^{1/3} M_n^{(1)}(i\omega_{n\xi}, \xi, x_2)\mathrm{Ai}(\pm|w|)\sin(\xi x_1 - \omega_{n\xi} t), \\ u_2 &\sim u_2^{(0)} - 2[\frac{2}{t|\omega_n'''(\xi)|}]^{1/3} M_n^{(2)}(i\omega_{n\xi}, \xi, x_2)\mathrm{Ai}(\pm|w|)\cos(\xi x_1 - \omega_{n\xi} t). \end{aligned} \tag{4.9}$$

Contributions from such points are called the 'Airy phases' and they become predominant at large values of time since they are proportional to $(t|\omega_n'''(\xi)|)^{-1/3}$.

We note that the above stationary phase analysis is valid only for finite stationary phase points. If ξ tends to infinity for some value of x_1/t then the approximation breaks down. From the asymptotic analysis of the dispersion relation (**11**) it is known that two stationary phase points, for the fundamental and higher modes respectively, are reached asymptotically at $k = \infty$. At these stationary phase points, the group velocity is equal to the velocity of the associated Rayleigh surface wave (Rayleigh-wave front) for the fundamental mode and it is equal to the velocity of the shear waves (the shear-wave front) for the higher modes. Jones (**8**) derived asymptotic expressions for both Rayleigh-wave front and the shear-wave front by considering the limiting forms of the integrands as $k \longrightarrow \infty$. However, recently, Dai and Wong (**9**) have pointed out that the calculations made by Jones for these two wavefronts are in error. Moreover, they have derived a uniformly valid asymptotic expansion for the shear-wave front. However, to derive a uniformly valid asymptotic expansion for Rayleigh-wave front remains an unsolved task.

In the next section, asymptotic results obtained from the above formulae will be compared with results from numerical integrations.

5. Numerical results

The integrals in (3.27) and (3.28) are evaluated numerically with the aid of Simpson's rule with the interval $(0, \infty)$ replaced by $(k_{\min}, k_{\max})$, where the constants $k_{\min}$ and $k_{\max}$ are chosen in such a way that results are not affected by decreasing $k_{\min}$ or increasing $k_{\max}$ further. For a reason which will be clear shortly, we decompose u_1 as

$$u_1 = u_1^{(0)} + u_1^{(1)} + u_1^{(n)}, \tag{5.1}$$

where

$$u_1^{(1)} = \frac{2}{\pi} \int_0^\infty M_1^{(1)}(i\omega_1, k, x_2) \cos\omega_1 t \sin k x_1 \, dk,$$

and $u_1^{(n)}$ can be obtained by comparing (5.1) with (3.27). It can be shown that the integrands in $u_1^{(0)}$ and $u_1^{(1)}$ behave like $\sin kx_1/k$ as $k \to 0$. This implies that the neglected integral from 0 to $k_{\min}$ is of order $k_{\min}x_1$ which increases as increasingly larger x_1 are considered. To avoid choosing increasingly small $k_{\min}$ to keep the error below a certain tolerant level, we may subtract the dominant terms from the integrands as follows.

First, it can be shown that as $k \to 0$,

$$M_1^{(1)}(i\omega_1, k, 1) = -\frac{1}{2v_0^2 k} + O(k), \quad \left(\frac{\Gamma_1}{\Gamma}\right)_{s=0} = -\frac{1}{v_0^2} + O(k^2), \tag{5.2}$$

where $v_0 = (\alpha + 3\gamma - 2\sigma_2)^{\frac{1}{2}}$ is the velocity of the fundamental mode at $k = 0$. We may then write

$$u_1^{(1)} = \triangle_1 + \frac{2}{\pi}\int_0^\infty \left(M_1^{(1)}(i\omega_1, k, x_2)\cos\omega_1 t + \frac{\cos kv_0 t}{2kv_0^2}\right)\sin kx_1\, dk, \tag{5.3}$$

$$u_1^{(0)} = \frac{1}{2v_0^2} - \frac{1}{\pi}\int_0^\infty \left\{\frac{1}{v_0^2} + \left(\frac{\Gamma_1}{\Gamma}\right)_{s=0}\right\}\frac{\sin kx_1}{k}dk, \tag{5.4}$$

where

$$\triangle_1 = -\frac{2}{\pi}\int_0^\infty \frac{\cos kv_0 t}{2kv_0^2}\sin kx_1\, dk = -\frac{1}{2\pi v_0^2}\int_0^\infty \frac{1}{k}\{\sin k(x_1 + v_0 t) + \sin k(x_1 - v_0 t)\}\, dk,$$

which is equal to 0 for $x_1 < v_0 t$, $-1/(4v_0^2)$ for $x_1 = v_0 t$ and $-1/(2v_0^2)$ for $x_1 > v_0 t$. The integrands in (5.3) and (5.4) now tend to zero as $k \to 0$, and if we replace the lower limit $k = 0$ of integration by $k = k_{\min}$ then it can be shown that the error is of order $k_{\min}^4 t^2$.

We now present our numerical results for the typical value $t = 40$ for which the results from the method of stationary phase may be used to validate our numerical results. After some experiments, we find that it is appropriate to choose $k_{\min} = 0{\cdot}01$, $k_{\max} = 40$, and a uniform step of 0·01 for the Simpson's rule. It is found that choosing a significantly larger $k_{\max}$ only affects the Rayleigh wavefront slightly and does not affect the wave profiles at other places. Figure 1 shows the two displacement components when only the fundamental mode (N=1) is included in the numerical evaluation and when the plate is stress free ($\sigma_2 = 0, \lambda = 1$). In order to get some feeling as to the meaning of these results, we examine the variation of the vertical displacement with x_1 at $x_2 = 1$, given in Fig. 1(b). As pointed out by Weaver and Pao (**5**), we can easily recognize three major features in Fig. 1(b). One feature is the early arrival of a relatively low amplitude and low frequency component. The next feature is the sharp spike of very high frequency appearing about $x_1 = v_R t \approx 38{\cdot}2$. The final feature is the late arrival of an exponentially decaying harmonic wave. All these features can be deduced qualitatively by using the method of stationary phase.

The results from the method of stationary phase are shown in Fig. 1(a,b) in dotted lines between $v_R t < x_1 < v_0 t$ and are obtained as follows. For each k which corresponds to a group velocity lying in (v_R, v_0), we calculate the corresponding $\omega_n(k)$, $\omega_n'(k)$, and $\omega_n''(k)$ from the dispersion relation (3.7). The value of x_1 is calculated according to $x_1 = \omega_n'(k)t$. Expressions in (4.6) can then be evaluated. We see that there is good agreement between numerical and asymptotic results. We note that far behind the waves u_1 has a non-zero value which should be the horizontal displacement when

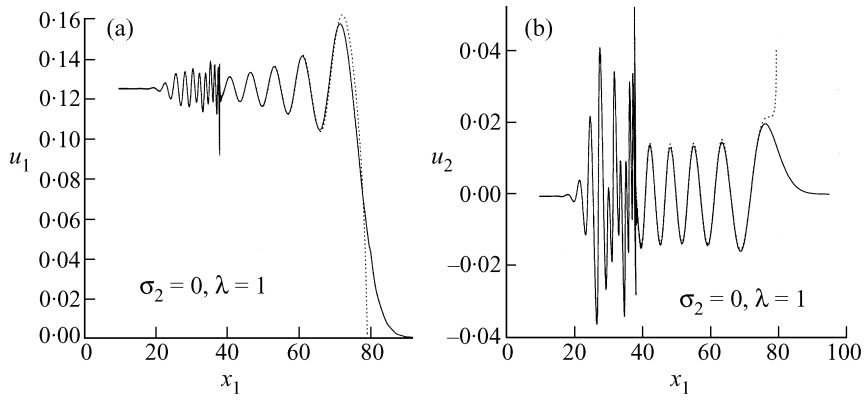

Fig. 1 Profiles of dispacement components at $x_2 = 1$, $t = 40$ when the plate is stress free ($\sigma_2 = 0, \lambda = 1$). Only the fundamental mode is included in the inversion integral. The dotted lines are the asymptotic results given by (4.6)

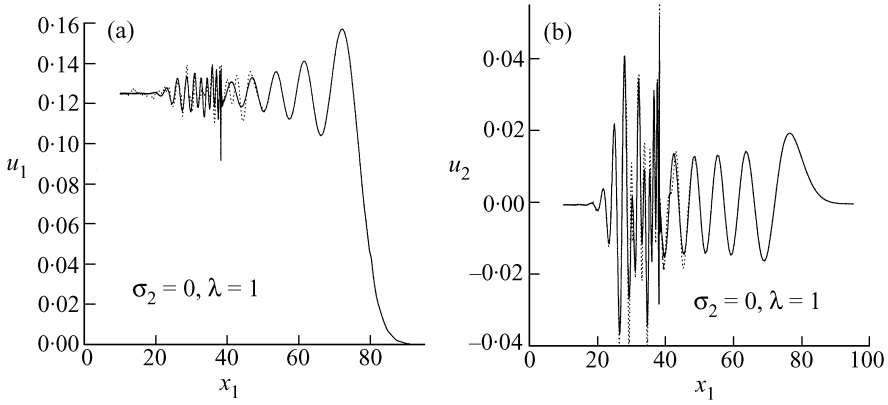

Fig. 2 Comparison between results of Fig. 1 and the corresponding results when five modes are included in the inversion integral. Solid line: one mode result (as in Fig. 1); dotted line: five mode result

the plate is subjected to a static line load. It can be deduced from (5.3) and (5.4) that this value is given by

$$u_1^{\text{static}} = \frac{1}{2v_0^2} = \frac{1}{2(\alpha + 3\gamma - 2\sigma_2)}. \tag{5.5}$$

This value can also be deduced using Betti's reciprocal theorem which states that for two sets of external forces acting on the same elastic body, the work done by the first set of force on the displacement caused by the second set of force is equal to the work done by the second set of force on the displacement caused by the first set of force. For the present problem, the first set of force is the static line load at $x_1 = 0, x_2 = 1$. The second set of force can be chosen to be a uniform traction $T_1^{\mathbf{n}} = 1, T_2^{\mathbf{n}} = 0$ on any cross-section $x_1 =$ constant $\neq 0$. We note from (5.5) the interesting result

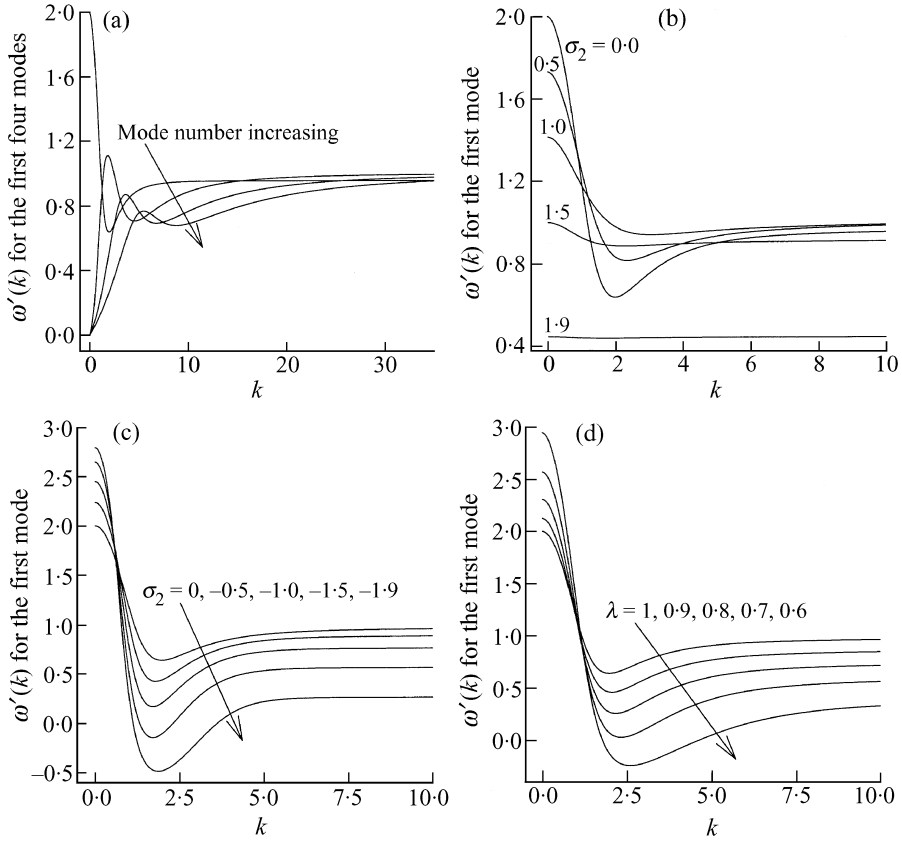

Fig. 3 (a) Group velocities of the first four modes when the plate is stress free ($\sigma_2 = 0, \lambda = 1$). (b) Group velocity of the fundamental mode for a selection of positive σ_2 values with $\lambda = 1$. (c) Group velocity of the fundamental mode for a selection of negative σ_2 values with $\lambda = 1$. (d) Group velocity of the fundamental mode for a selection of λ values with $\sigma_2 = 0$

that when $\lambda = 1$ (so that $\alpha = \gamma = 1$), we have $u_1^{\text{static}} \to \infty$ as $\sigma_2 \to 2$, the latter limit being a buckling all round tension, see (3.8).

Figure 2 shows a comparison between results obtained by including five modes and those of Fig. 1. It can be seen that higher modes affect the waves behind the Rayleigh wavefront quantitatively but do not change the overall structure of the whole wave profile. We find that results obtained by including more than five modes are graphically indistinguishable from those in Fig. 2. Thus all of the following numerical results are obtained by including five modes.

In Fig. 3(a) we have shown the dependence on k of the group velocities (c_g) for the first four modes and for the case when the plate is stress free. To relate such dependence to the asymptotic results presented in Fig. 1(b), we note that there are three stationary phase points associated with the fundamental mode which are of special interest. The first one corresponds to $c_g = v_0 = 2$ and $k = 0$. A group moving at this speed would appear around $x_1 = 80$ when $t = 40$ (see Fig. 1(b)). The second one corresponds to a local maximum at infinite wavenumber, with $c_g = v_R$. This

appears as the sharp Rayleigh peak at $x_1 = 38{\cdot}2$ in Fig. 1(b). As a matter of fact this peak ought to be of infinite height (see the discussion at the end of section 3). But a high-wavenumber truncation in our numerical calculations ($k_{\max} = 40$) eliminates this singularity. Finally, there is a minimum at a moderate wavenumber, $k \approx 1{\cdot}98$. Correspondingly we expect an Airy phase like contribution which appears as the exponentially decaying harmonic wave in Fig. 1(b).

With the use of the method of stationary phase explained in the previous section, we deduce that waves have negligible amplitude in the region ahead of the wavefront $x_1 = v_0 t$. Between $x_1 = v_0 t$ and $x_1 = v' t$, where v' is the first maximum in Fig. 3(a) as we move down from $c_g = v_0$, the displacement field is well approximated by the asymptotic results (4.6), as can be seen in Fig. 1. Behind the wavefront $x_1 = v' t$, there is more than one point of stationary phase and each term of the summation in equation (4.6) must include a further summation over all the stationary phase points of the corresponding branch.

Figures 3(b, c, d) show the variation of the group velocity of the fundamental mode with respect to σ_2 and λ. These graphs provide us with a rough idea about how fast the wavefront $x_1 = v_0 t$ propagates and over which region the one-term asymptotic results (4.6) are expected to provide good approximations. We note that when the plate is subjected to a uni-axial compression or an all-round pressure, the group velocity can become negative when the compression or pressure is big enough. We will see shortly that a consequence of a negative group velocity is that waves do not propagate away from the point of impact.

Figures 4(a, b, c, d) show the profiles of surface elevation when the plate is subjected to an all-round tension with $\lambda = 1$ and $\sigma_2 = 0{\cdot}5, 1{\cdot}0, 1{\cdot}5, 1{\cdot}9$. We see that as the all-round tension is increased gradually from zero, the Rayleigh wavefront becomes more and more dominant and it has increasingly greater amplitude. Figure 4(d), which corresponds to $\sigma_2 = 1{\cdot}9$, shows only a single peak. As we remarked earlier, the Rayleigh wavefront is sensitive to the choice of $k_{\max}$. Figure 4(d) also shows a comparison between results obtained by taking three different truncation numbers $k_{\max} = 40, 60, 80$. We see that choosing a larger $k_{\max}$ gives a larger amplitude for the Rayleigh wavefront, but the shapes of the profiles remain qualitatively the same. We also note that $\sigma_2 = 2$ is the critical value for buckling instability. At this critical value, the plate behaves like a non-dispersive medium in the sense that the group velocity, which is zero, is independent of the wavenumber. Figure 4(d) demonstrates that as σ_2 approaches this critical value, energy becomes increasingly concentrated on the Rayleigh wavefront. Some of these results could also have been anticipated from an inspection of Fig. 3(b). We see that as the tension increases, the profile of group velocity becomes increasingly more and more flat, which, together with our earlier discussion of evaluation of integrals by the method of stationary phase, implies that energy should be concentrated in an increasingly narrow region and propagate at an increasingly slow speed. Although it is not meaningful to compare the Rayleigh wavefronts since they should have an infinite amplitude, we note, however, that in Fig. 4(c) the peak ahead of the Rayleigh wavefront has a much larger amplitude than its counterparts in Figs 4(a,b).

If σ_2 is increased beyond the critical value of 2, exponential growth will occur. The further behaviour of the impact waves can only be assessed with the aid of a nonlinear analysis.

Figures 5(a, b, c, d) show the profiles of surface elevation when the plate is subjected to increasingly larger all-round pressure: $\sigma_2 = -0{\cdot}5, -1{\cdot}0, -1{\cdot}5, -1{\cdot}9$. These figures should be read in conjunction with Fig. 3(c) which shows that v_0, the speed of the foremost wavefront, increases as the pressure is increased. In contrast with the case of increasing all-round tension, there is a scatter of energy over a long range and waves do not propagate away from the point of impact,

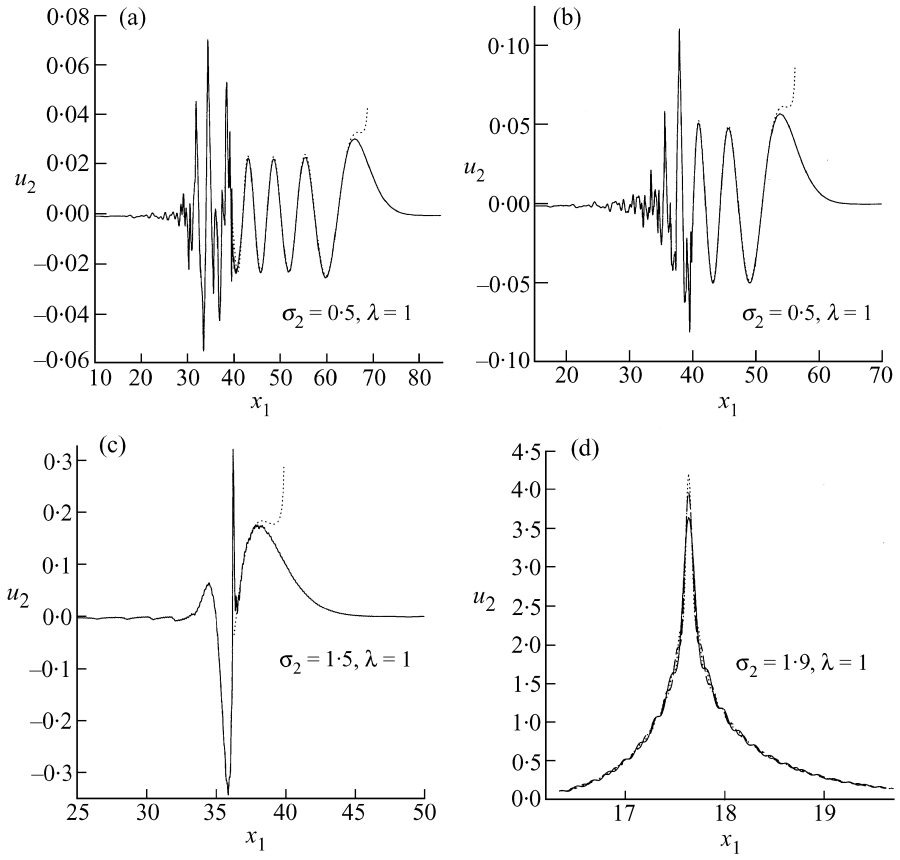

Fig. 4 Surface elevation when $t = 40$ and the plate is subjected to an all-round tension. (a) $\sigma_2 = 0{\cdot}5$; (b) $\sigma_2 = 1{\cdot}0$; (c) $\sigma_2 = 1{\cdot}5$; (d) $\sigma_2 = 1{\cdot}9$. The dotted lines in (a)-(c) are the asymptotic results given by (4.6). In (d), results corresponding to $k_{\max} = 40, 60, 80$ are shown; a larger truncation number corresponds to a higher peak

corresponding the occurrence of negative group velocities. In this case it is the peaks behind the Rayleigh wavefront that have increasingly large amplitudes as the pressure is increased.

Finally, Figs 6(a, b, c, d) show the profiles of surface elevation when the plate is subjected to increasingly larger uni-axial compression: $\sigma_2 = 0$ and $\lambda = 0{\cdot}9, 0{\cdot}8, 0{\cdot}7, 0{\cdot}6$. These figures should be read in conjunction with Fig. 3(d) which shows the profiles of group velocity for the same λ values. We see that increasing the uni-axial compression has similar effects to increasing the all-round pressure: the foremost wavefront travels increasingly fast, there is a scatter of energy over a large range, and the peaks behind the Rayleigh wavefront have increasingly large amplitudes. We have not considered the effects of uni-axial tension since a neo-Hookean plate cannot buckle under uni-axial tension.

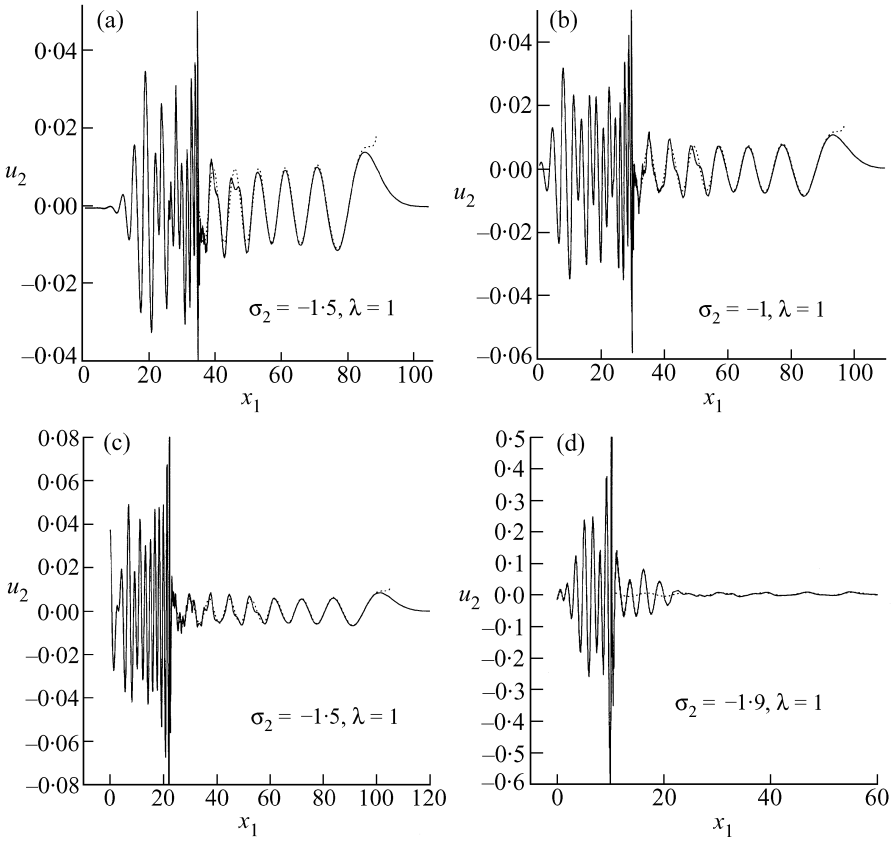

Fig. 5 Surface elevation when $t = 40$ and the plate is subjected to an all-round pressure. (a) $\sigma_2 = -0{\cdot}5$; (b) $\sigma_2 = -{\cdot}0$; (c) $\sigma_2 = -1{\cdot}5$; (d) $\sigma_2 = -1{\cdot}9$. The dotted lines are the asymptotic results given by (4.6)

6. Conclusions

In this paper we have studied impact waves resulting from an application of a sudden line load to the surface of a pre-stressed elastic plate placed on a smooth foundation. The pre-stress takes the form of a uni-axial compression or an all-round pressure (tension). Such a plate becomes unstable if the all-round pressure (tension) satisfies (3.8) or if the uni-axial compression satisfies (3.10). Our interest has been in the behaviour of these impact waves as the pre-stress approaches its buckling values. It is found that a uni-axial compression and an all-round pressure have similar effects on the impact waves. As the compression or pressure is increased gradually towards its buckling value, negative group velocity can be achieved and waves do not propagate away from the impact point. Waves of increasingly large amplitude behind the Rayleigh wavefront are also observed. When the plate is subjected to an all-round tension, the impact waves behave quite differently. Group velocity never becomes negative and waves propagate away from the impact point. As the tension approaches twice the shear modulus, the critical value for buckling instability for all wavenumbers,

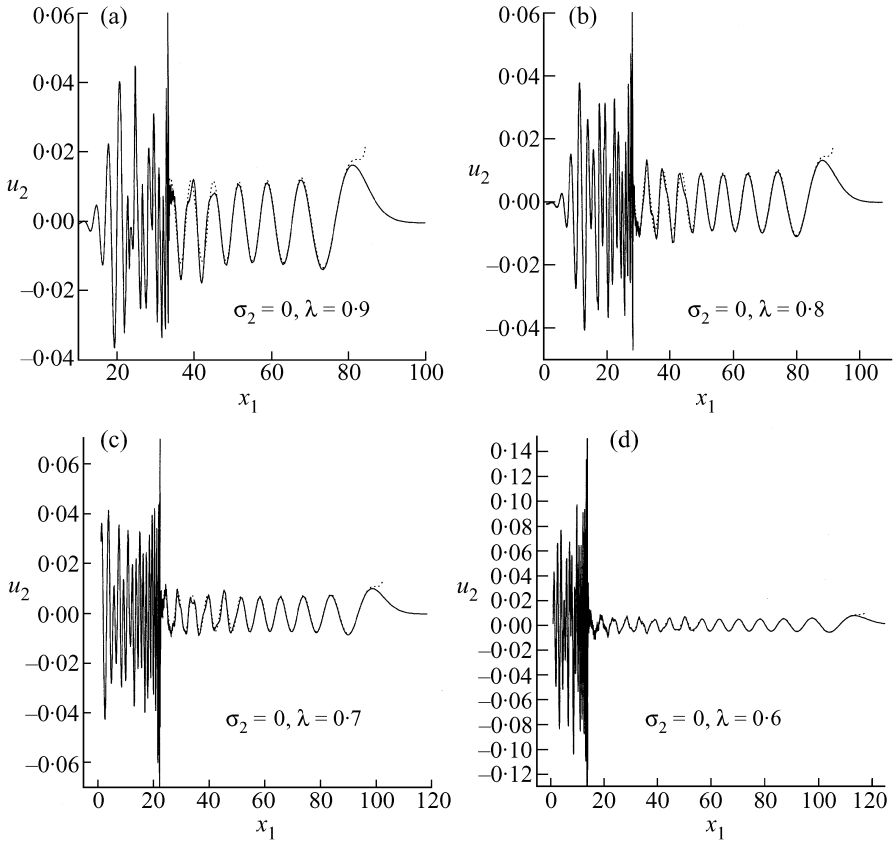

Fig. 6 Surface elevation when $t = 40$ and the plate is subjected to a uni-axial compression. (a) $\lambda = 0{\cdot}9$; (b) $\lambda = 0{\cdot}8$; (c) $\lambda = 0{\cdot}7$; (d) $\lambda = 0{\cdot}6$. The dotted lines are the asymptotic results given by (4.6)

energy becomes increasingly concentrated near the Rayleigh wavefront and the waves propagate away from the impact point almost as a single peak wave at an increasingly small speed.

Acknowledgements

The paper was written when the first author was visiting the Department of Mathematics of the University of Manchester. He acknowledges the support by the Royal Society and TUBITAK (of Turkey) through the European Science Exchange Programme. Useful discussions with Professor J. D. Kaplunov and Dr Z. X. Cai are also gratefully acknowledged.

References

1. R. D. Mindlin, *An Introduction to the Mathematical Theory of Vibrations of Elastic Plates* (U.S. Army Signal Corps Engineering Laboratories, Fort Monmouth, NJ 1955).
2. J. Miklowitz, *The Theory of Elastic Waves and Wave Guides* (North–Holland, New York 1978).
3. J. D. Achenbach, *Wave Propagation in Elastic Solids* (North–Holland, Amsterdam 1990).

4. F. Santosa and Y.-H. Pao, Transient axially symmetric response of an elastic plate. *Wave Motion* **11** (1989) 271–295.
5. R. L. Weaver and Y.-H. Pao, Axisymmetric elastic waves excited by a point source in a plate. *ASME J. appl. Mech.* **49** (1982) 821–836.
6. W. A. Green and E. R. Green, Stress variation due to an impact line load on a 4-ply fiber composite plate. *Int. J. Sol. Str.* **28** (1991) 567–594.
7. G. A. Rogerson, Penetration of impact waves in a six-ply fibre composite laminate. *J. Sound Vib.* **158** (1992) 105–120.
8. P. N. Jones, Transverse impact waves in a bar under conditions of plane-strain elasticity. *Q. Jl Mech. appl. Math.* **17** (1964) 401–421.
9. H.-H. Dai and R. Wong, A uniform asymptotic expansion for the shear-wave front in a layer. *Wave Motion* **19** (1994) 293–308.
10. R. W. Ogden and D. G. Roxburgh, The effect of pre-stress on the vibration and stability of elastic plates. *Int. J. Engng Sci.* **31** (1993) 1611–1639.
11. G. A. Rogerson and Y. B. Fu, An analysis of the dispersion relation and dynamic stability of a pre-stressed incompressible elastic plate. *Acta Mech.* **111** (1995) 59–74.
12. P. Chadwick, *Continuum Mechanics: Concise Theory and Problems* (Allen & Unwin, London 1976).
13. R. W. Ogden, *Non-linear Elastic Deformations* (Ellis Horwood, New York 1984).
14. Y. B. Fu and G. A. Rogerson, A nonlinear analysis of instability of a pre-stressed incompressible elastic plate. *Proc. R. Soc.* A **446** (1994) 233–254.
15. ——, A nonlinear stability analysis of an incompressible elastic plate subjected to an all-round tension. *J. Mech. Phys. Solids* **46** (1998) 2261–2282.
16. —— and R. W. Ogden, Nonlinear stability analysis of pre-stressed elastic bodies. *Continuum Mechanics and Thermodynamics* **11** (1999) 141–172.
17. R. Wong, *Asymptotic Approximations of Integrals* (Academic Press, London 1989).
18. M. Abramowitz and I. A. Stegun (eds), *Handbook of Mathematical Functions* (Dover Publications, New York 1970).